Aerosol and Air Quality Research, 1678–1692, 2013

ISSN: 1680-8584 print / 2071-1409 online
doi: 10.4209/aaqr.2013.02.0039

Evaluation of the Airborne Particles Fraction Responsible for Adverse Health Effects

Boris Gorbunov[1], Robert Muir[1*], Philip Jackson[2], Nicholas D. Priest[3]

[1] *Naneum, CIC, University road, Canterbury, Kent CT27FG, UK*
[2] *CERAM Research, Queens Road, Penkhull, Stoke-on-Trent, Staffordshire ST4 7LQ, UK*
[3] *Atomic Energy of Canada Ltd, Chalk River, Ontario, K0J 1J0, Canada*

ABSTRACT

A new approach to evaluation of the fraction of airborne particles that is responsible for adverse health effects has been developed. In this approach a two-fraction concept for the adverse health effects is proposed. This concept considers aerosol particles in the air, the fraction of particles deposited in the respiratory system (captured by the system) and the fraction of particle accumulated in the body (captured by the body). The latter fraction of airborne particles actually causes the adverse health effects and associated with the health risk. The approach has been applied to workers in crystal glass industry exposed to lead. A size resolved sampling technique was employed to characterize nanoparticles at work places at several plants involved in lead processing. Lead aerosol size distributions were obtained across the entire aerosol particle size range from 1 nm to 30 μm (diameter). Size distributions were used to calculate the total lead intake due to particle deposition in the respiratory system of workers. A bio-kinetic model was employed to evaluate various size fraction contributions to the total blood lead level in workers. A comparison was made between calculated blood lead levels and actual measurements of blood lead levels of workers exposed to atmospheres containing lead. It was found that nanoparticles cause the major health risk due to high deposition efficiency and low clearance rate by the mucociliary escalator.

Keywords: Lead; Nanoparticles; Lung deposition; Exposure.

INTRODUCTION

Numerous epidemiological studies have shown associations between exposure to particulate matter in the air and increases in morbidity and mortality Brown *et al.* (2002); Dockery *et al.* (1993); Pope *et al.*(1995), etc. Long lasting inflammation is an important mechanism for adverse health effects following exposure to nanoparticles. There is a growing concern that nanoparticles (less than 100 nm in diameter) have an increased toxicity relative to larger particles composed of the same materials, e.g., Ferin *et al*. (1992); Ferin (1994); Oberdorster *et al*. (1995); Donaldson *et al*. (1998). This could be explained by transfer of toxic substances through the blood stream or by particles crossing other membranes in the respiratory tract. There is evidence supporting this in animal studies Obersdorster *et al.* (2003), but as yet no direct evidence of particles passing from the respiratory tract into the blood stream from studies of human exposure to well characterised airborne particles.

Quantification and management of the health risks caused by exposure to toxic particles in air are important issues that many industries face. These problems occur where nanoparticles are by-products of manufacturing processes such as incineration, smelting, welding and others. There is also increasing awareness of health risks that may occur with the production and commercialisation of novel nano-materials where specific properties are engineered into the material at the nano-scale. There is concern that the enhanced properties engineered into the material will also impact biological activity and toxicity, increasing the health risks posed by these new materials.

Currently exposure level is evaluated using total mass concentrations of material of concern in a size range below a certain cut off diameter, for example 10 μm (PM_{10}) and 4 μm (the respirable fraction).

The specific dose of particles accumulated in humans as a result of exposure to airborne particulate matter is poorly characterised. The main pathway for airborne particulate matter to enter the body is via the respiratory system. The accumulated dose as a result of exposure to airborne particles does not just depend on the concentration of particles in the air, but is a result of the interplay of a number of factors including the deposition efficiency of

* Corresponding author.
Tel.: 44-1227-811-705; Fax: 44-1227-811-701
E-mail address: robert.muir@naneum.com

particles in the respiratory tract and the bioavailability of those particles once they have deposited.

Particles in the air are characterised by size distribution functions, for instance particle number size distributions, surface area size distributions and particle mass size distributions, see for instance Hinds (1999) or John (2001). Often distributions are quite complicated. There are observations of bi-modal and three-modal particle size distributions, e.g., Whitby (1978) and Gorbunov *et al.* (2010). Particle size distributions are influenced by the sources and sinks of aerosol particles, the history of the air mass as well as the meteorological and local conditions. Thus, distributions are different in different environments and are subject to temporal and spatial variations.

Exposure to air containing particulate matter leads to deposition of some particles in the respiratory system. Deposition of particles in the human respiratory system is a complex phenomenon that involves many physical and chemical processes including diffusion, interception and the inertial properties of particles. Diffusivity and the inertia of particles depend upon their size, e.g., Gnewuch *et al.* (2009). Total and regional deposition of particles of various sizes in airways were calculated using numerical models often based on fluid dynamics, e.g., Finlay and Martin (2008), Longest and Holbrook (2012); Kleinstreuer *et al.* (2008). Deposition in tracheobronchial or alveolar regions is different for nanoparticle and for submicron particles. Submicron and larger particles are captured mainly in head-airways. Nanoparticles, however, can penetrate into the alveolar region. It was observed that there are some highly localised areas "hot spots" where deposition density was many times greater than in the vicinity of the spots, see for example Phalen *et al.* (2006); Xi and Longest (2008). Hot spots facilitate particle agglomeration in airways but it is not clear how this affects particles bioavailability. In general, there is a lack of experimental *in vitro* and *in vivo* data to validate highly localised modelling predictions, Holbrook and Longest (2012).

In addition, some particles after being deposited are removed from the respiratory system to the stomach as a result of clearance mechanisms and swallowing, Appendix A.

The number size distribution of particles deposited in respiratory system $N_d(D)$ is a product of the ventilation rate Q, exposure time t, airborne particle size distribution $f_a(D)$ and the deposition efficiency of aerosol particles $E(D)$

$$N_d(D) = Q\, t f_a(D)\, E(D) \tag{1}$$

$N_d(D)$ represents the number distribution of particles that were captured by the respiratory system and D is the particle diameter. The efficiency of deposition in the respiratory system was subject to experimental research and modeling and widely available, e.g., Chamberlain (1985); Anjilvel and Asgharian (1995); Lippmann (1995); Yeh *et al.* (1996); Hinds (1999); Asgharian *et al*. (2001); Holbrook and Longest (2013).

It was found that the deposition efficiency was influenced by particle sizes and varied from 10 to 100%. Thus, exposure to nanoparticles is governed to a large extent by particle size. This is equally true for soluble particles, exposure to toxic substances associated with particles and for insoluble particles. Insoluble particles can cause adverse effects after pulmonary deposition due to long lasting retention and inflammation.

It is important that not all the particles deposited in the respiratory system contribute to adverse health effects and toxicity. Some particles are removed from the respiratory system by the mucociliary escalator processes. The removal of particles by cleaning mechanisms is influenced by size, e.g., Oberdörster *et al.* (1994); Koch and Stöber (2001). Clearance by the mucociliary escalator mechanisms are less effective for smaller particles than for larger particles. Smaller insoluble particles require a much longer time, to be removed from the lungs and upper respiratory tract possibly because of deposition in different regions of the respiratory tract such as the alveolar region.

Finally, the size distribution of accumulated particles relevant to health risk $N_h(D)$ can be expressed via the fraction of particles remaining in the body or the bio-available fraction $A(D)$. These particles cause actual adverse health effects.

$N_h(D)$ is a product of $A(D)$ and the size distribution of particles (1) deposited in the respiratory system

$$N_h(D) = Q\, tA(D)\, E(D)\, f_a(D) \tag{2}$$

$N_h(D)$ is the differential form of the body burden representing the number of particles of concern related to a certain size range D to $D + dD$. The total body burden is therefore the integral of expression (2).

$$N_h = Q_t \int_{D_{\min}}^{D_{\max}} A(D)E(D)f_a(D)dD \tag{3}$$

N_h represents the total number of particles accumulated in the body after an exposure for time t to an aerosol with the size distribution $f_a(D)$. $D_{\min}$ is normally 1 nm and $D_{\max}$ is the maximal size that is practically important as far as health risk is concerned. The value of the $D_{\max}$ can be accepted as the respirable cut off size (4 μm). In practice, it is subject to special consideration related to the micro-environmental conditions such as wind speed and the breathing pattern of workers. However, it has to be remembered that $E(D)$ decreases when diameter of particles become greater than 4 μm, Hinds (1999). Thus variation in the upper limit of integration in expression (3) does not affect the total body burden considerably.

This expression is valid for any particle size distribution: number, surface area or mass. For a particle of any size there are two main channels that remove some inhaled particles on the way from the air to body compartments, Fig. 1. This Figure illustrates the importance of taking into account all processes to evaluate health risks associated with exposure to airborne particles.

According to expression (3) derived from the principle of the mass conservation law the link between the aerosol in the air (cause) and the adverse health effects (result) is influenced by the aerosol particle size distribution, the

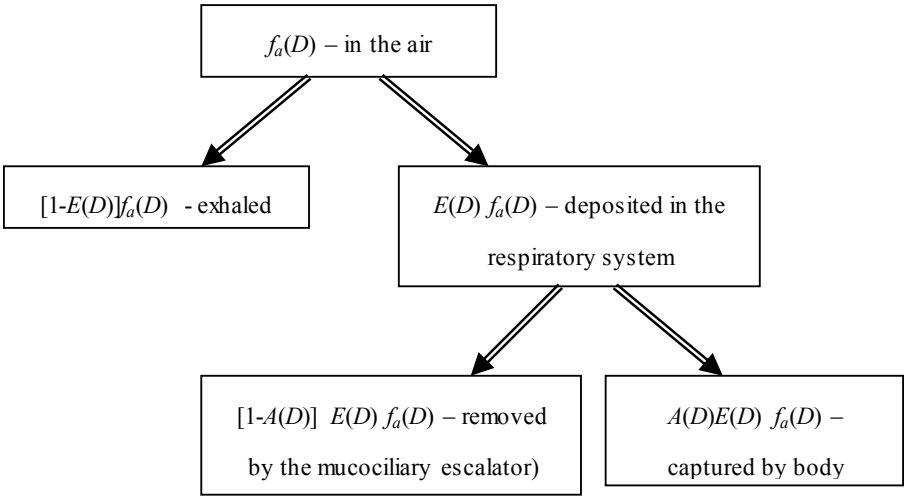

Fig. 1. Aerosol particle pathways from the air to body organs. $f_a(D)$ is aerosol particle size distribution in the air. $E(D)$ is the deposition efficiency of aerosol particles in the airways. $A(D)$ is the bioavailability fraction.

deposition efficiency of particles in the respiratory system and the fraction responsible for the adverse health effects (bioavailability). It also depends on time and the respiratory ventilation rate. Aerosol particle size distributions can be measured with a wide range aerosol sampling system such as Nano ID Select (PMS Inc.), Gorbunov *et al.* (2009). Aerosol particle deposition efficiency was studied extensively in the past, e.g., ICRP (1994), Anjilvel and Asgharian (1995), Asgharian *et al*. (2001), Holbrook and Longest (2013).

The respiratory system ventilation rate was also studied earlier, e.g., ICRP (1975). Much less is known about toxic fractions of particles deposited in the respiratory system.

It is likely that $A(D)$ is different for humans and rodents or other mammals. Therefore, evaluation of it requires information from human subjects.

An opportunity to determine the hazardous fraction ($A(D)$) recently arose in the crystal glass industry. This study was motivated by blood lead bio-monitoring data in workers in some European crystal glass factories. The measured blood lead levels did not correlate well over time with measured airborne respirable (inhalable) lead levels and the personal protection measures taken seemed to have little effect. It was therefore hypothesized that workers were being exposed to lead in the nano-size range and that this fraction was making a significant and disproportionate contribution to the body burden of lead rather than simply the total respirable mass.

Commonly, a measure of exposure to lead of workers was based on mass of lead in the air collected onto an aerosol filter with size selective inlets such as PM_4 and $PM_{2.5}$ and measured with off-line chemical analysis. This implies that it was assumed that $A(D) = 1$ and $E(D) = 1$ over the entire size range defined by size selective inlets. The validity of these assumptions is not fully understood especially in the crystal glass industry where furnaces can potentially generate lead nanoparticles.

The aim of this paper was to develop a new approach for Health Risk evaluation based upon quantification of the Accumulated Dose (HR-AD) using lead exposure data obtained at various factories over the entire airborne particle size range. This approach was focussed on a study of workers exposed to lead containing particles produced as a by-product of the manufacturing processes in the European crystal glass industry (in European countries).

METHOD

HR-AD Approach Methodology

There is no direct way of finding hazardous fraction function. An estimate of $A(D)$ function proposed in this paper is based upon a comparison of blood lead contents in workers. On the one hand, the lead content was measured in blood of workers. On the other hand, the blood lead content was calculated from measured airborne lead particle size distributions $f_a(D)$, known $E(D)$, a bio-kinetic model that determines exchange rates of lead between various body compartments including blood and a parameterised hazardous effects function $A(D, par)$. Here the hazardous fraction is determined by a set of unknown parameters (par). $A(D, par)$ is simply a representation of $A(D)$ determined above to emphasise the way of finding this function by variation of the parameters. According to HR-AD approach we found parameters characterising $A(D)$ function by comparison the measured lead content in blood and calculated values. The set of parameters was varied to minimise the difference between the measured and calculated data. Parameters providing the minimal difference between measured and calculated blood lead content were accepted to determine an evaluation of the adverse health effects fraction $A(D)$.

In this paper the proposed approach for health risk evaluation was applied to the crystal glass industry. Data on aerosol particle size distributions and blood lead concentration were collected at working places at several European factories processing lead and lead compounds both mechanically and chemically, including high temperature stages. In addition, we investigate the hypothesis that significant airborne lead exposure in the nano-size fraction is generated in crystal glass factories and we clarify the role of nanoparticles in the total lead body burden.

An area sampling approach was adopted, in part because efficient personal samplers for nanoparticles were not (and still are not) available at the time of the study.

The HR-AD method requires three sets of data: the aerosol particle size distributions $f_a(D)$, deposition efficiency in the respiratory system $E(D)$ and a calculated level of lead in blood derived from a lead bio-kinetic model.

A validated bio-kinetic model of lead metabolism in humans (ICRP, 1975; Leggett, 1993) was employed to predict blood-lead levels in workers exposed to lead aerosols. The deposition efficiency of aerosol particles in the respiratory system was taken from Hinds (1999) and ICRP (1994). Although there are other models available, e.g., MPPD model for aerosol deposition estimation in human lung, see Anjilvel and Asgharian (1995), the choice of ICRP was motivated by its compatibility to an available bio-kinetic model of lead metabolism in humans. Particulate matter size distributions were obtained with recently developed wide range size resolved aerosol sampler Nano ID Select.

Manufacturing Stages of Crystal Glass

Lead crystal glass contains a minimum lead oxide content of 24%. Production of the crystal glass comprises several stages-mixing of raw materials, melting, shaping of molten glass, annealing, polishing, and cutting/decorative. These steps usually take place in different locations (departments) within a factory.

The initial stage of the process is the provision and mixing of the raw materials, which include SiO_2, B_2O_3, Al_2O_3, MgO and PbO. The mixture is then fed into melting pots, which are normally heated in furnaces to an operating temperature from 1,100 to 1,200°C. Several pots are often run in parallel. The molten glass from the furnace is then forced into a shape by air pressure (either by hand blowing or machine). Blowing requires the crystal glass piece to be at 400–600°C. Blowers are typically situated in close proximity to furnaces, e.g., around them. The next step in the process is annealing. During annealing, shaped pieces move slowly (over three hours) along a horizontal tunnel (~20 m long) through a decreasing temperature gradient, passing gradually from a higher temperature of a few hundred degrees to room temperature. The glass objects then undergo polishing, which involves immersing glass pieces in a vat containing a mixture of hydrofluoric and sulphuric acids for a short time. Finally, the glass objects are decorated with different patterns which are carved onto the piece with carborundum wheels.

The main processes in a crystal glass production factory believed to generate the highest airborne lead exposures involve melting and blowing of hot molten glass (in and around the furnace areas) which may lead to the formation of lead containing nanoparticles via nucleation processes, as and decorative patterning of glass using grinding wheels. Cutting may generate a broader range of size distributions of larger lead particles. The size distribution of airborne lead particles down to nano-size range has not been quantified.

Sampling Sites and Processes

Sampling sites were chosen at 4 different crystal glass factories at various stages of production, and, as mentioned previously, targeted the furnace and cutting departments. Polishing was also included into the sampling sites for comparison purposes. In all, we sampled the furnace departments in two sites, cutting departments in three sites, and polishing departments in two sites. The duration of sampling was normally 8-hours (one shift). However, in cases of very low concentration of lead in the air, the duration was longer.

An example of a typical furnace department configuration is shown schematically in Fig. 2. Six ovens that contain melted crystal glass at high temperature were arranged along the perimeter of a circle in the middle of the furnace area. Each furnace (C) was equipped with an individual extraction (D) of the local ventilation system (canopy hood type). In the furnace areas, several doors and windows were kept opened at all times. A large industrial door (Door 1) in the area was kept open all year round. Normally 15 to 45 workers, working in three shifts (5 to 15 workers per shift) were in the area involved in crystal glass production and were exposed to the lead aerosol. The furnaces areas were not directly connected to the cutting and grinding areas but some lead aerosol escaped from the furnaces area can travel to other areas and contribute to the lead exposure. In two furnace areas (about 450 m^2 and 520 m^2 in size) samples were collected in February of 2000.

In three cutting departments (340, 250 and 200 m^2) samples were collected in February and in May of 2000. Normally, 20 to 35 workers working in one shift were exposed to lead aerosols in these departments. Workers spent nearly all the work shift (~7.5 hrs) sitting at their workbenches in front of cutting wheels. Workplaces were equipped with running water and personal protection (screens). Thus workers were exposed to the aerosol in this area on a daily basis for at least 7 hrs/week five days a week for about 11 months a year. Most of the workers were permanent employees.

A typical example of the cutting department has two rows of cutting workers sites where up to 20 workers can work at the same time, (Fig. 3). All windows and doors were normally closed. A local ventilation system was continuously active.

In two polishing departments (about 80 m^2 and 180 m^2) samples were collected in December 1999. In the polishing departments the number of involved workers was smaller: 5 to 10. However, all the departments were interconnected, allowing for possible transport of airborne lead aerosols to different areas of the facility. The polishing stations were also equipped with local exhaust ventilation (canopy hoods).

The production cycle and work load was reported as largely constant over several years prior to the sampling campaign. The sampling time was chosen by industrial partners to represent the typical situation.

Comparison of Personal and Area Sampling

Natural air convection in large internal spaces and local ventilation are likely to have mixed air masses in all departments. However, open windows and doors create additional inflow and outflow of the air and may create differences in lead aerosol concentration. The location of the integrated area samplers (NanoID Select) was guided by

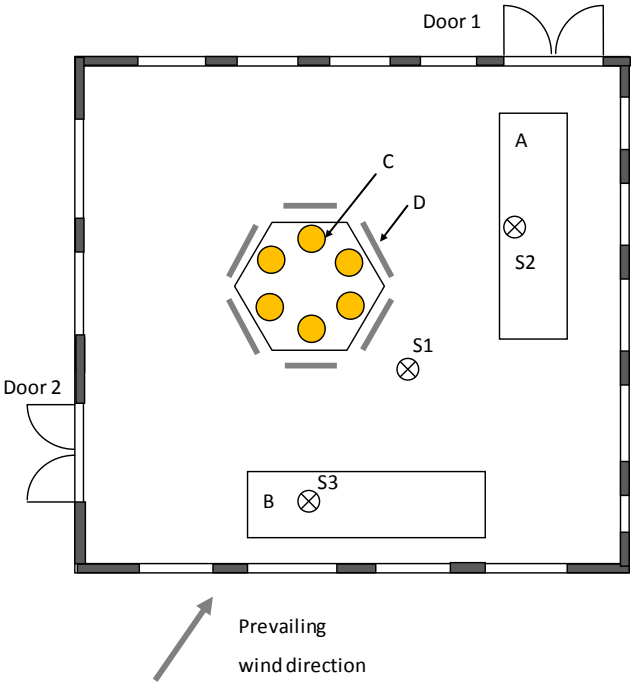

Fig. 2. Schematic of the furnace area including blowing areas (A and B).The furnaces shown with circles (C). Extraction air inlets positioned above the furnaces are shown with a wide gray lines (D). Sampling sites are S1, S2 and S3.

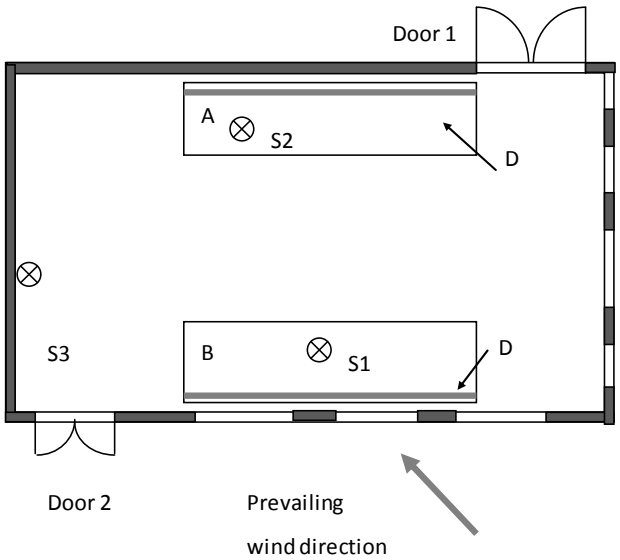

Fig. 3. Schematic of the cutting area (A and B). Sampling sites are S1, S2 and S3. Extraction of the local ventilation system is shown as D.

the geometry of the area and workers' location in relation to the point sources. Preliminary stationary area sampling for $PM_{2.5}$ (described below) was used to assess spatial variability on lead air concentrations in the furnace and cutting departments and define the final position of the NanoID sampler.

In all departments, occupation hygienists in the facility used personal samplers (as stationary samplers) operating at 2.0 L/min and equipped with a cyclone with a cut off size 2.5 μm (Casella Ltd.). These samplers were used to find the most representative location for the Nano ID Select. OH samplers enable all the particles up to 2.5 μm to be collected onto 25 mm aerosol PTFE fibre filters (WRR), part number R2PI025). OH samplers were stationary, positioned at the height of 1.6 m in the furnace and polishing departments (3 m from the furnace entrance) and at 1.2 m in the cutting areas where workers were sitting at workbenches, in such a way that they would serve as surrogate measures of personal exposures. The sampling time was for the whole duration of the 8-hr shift.

The total mass concentration of airborne particles collected with the OH samplers was determined gravimetrically (as a

post-pre weight difference using a microbalance (XP6 Microbalance, Mettler) with a resolution of 0.1 μg (limit of detection 1 μg). Airborne $PM_{2.5}$ concentrations were found to be in the range from 20 to 110 μg/m^3. Lead content determined with ICP and AAS was in the range from 0.5 to 1.1 μg/m^3. In total 48 samples were quantified.

In addition to the preliminary OH sampling assessment, one OH sampler was stationary positioned next to Nano ID-Select during the sampling campaign for inter-comparison purposes (nine pairs in total). Comparison of Nano ID-Select mass concentration related to 2 μm cut off diameter (sum of the 1st through 8th stages) with OH sampler data gave an agreement of ±28%. This may be caused by difference in the 50% cut off sizes (2.5 μm for OH sampler and 2.0 μm for Nano ID Select), as well as differences in the penetration efficiencies for both samplers. For example, penetration efficiency for a cascade impactor (Nano ID Select) is considerably steeper than the penetration efficiency for a cyclone (OH sampler).

Sampling time for Nano ID Select was rather limited by the logistics of the project. The agreement of Nano ID Select data with OH sampler data (including preliminary data) was important evidence supporting the choice of sampling sites.

The sampling strategy was based on preliminary investigation of the spatial and temporal variability of lead at the working places and the choice of the most representative location and a sampling time as close as possible to the average scenario of exposure. The OH sampler pool of data was much greater than Nano ID data set and the time span was considerably longer. It is also important that spatial and temporal variability of OH sampler data were investigated before Nano ID data were obtained. Good agreement with OH sampler data confirmed that the Nano ID data represented typical exposure scenarios at the working places studied and therefore can be used in correlation research with the blood level of lead in workers.

Blood Lead Analysis

Venous blood was collected from workers twice a year as part of the lead monitoring program by the companies in accordance with the Health and Safety Executive (UK) recommendations. The UK standard is equivalent to the USA OSHA lead standard, 29 CFR 1910.1025. Blood samples were kept in lead free containers. Sample preparation was performed in a clean environment, in accordance to International Organisation for Standardisation class 5 setting. The total number of workers involved in blood lead screening was 95 (45 – furnace areas, 35 – cutting and 15 – polishing). Workers were chosen to represent a typical age for the site (normally with employment records of between 5 and 15 years). Lead in blood was analyzed according to method (1910.1025) using atomic absorption spectroscopy with Zeeman background correction according to EURACHEM guidelines and quality control. Briefly, blood is hydrolyzed with HCl to release Pb from red blood cells RBC, diluted, and analyzed by Atomic Adsorption Spectroscopy AA using standard wet chemistry analytical techniques. The standardized method gives a limit of Pb detection in a sample 1 μg/dl, repeatability of 8%. 5% of samples were below the limit of detection. Statistical analysis was performed using the SPSS 9.0 Statistical Package for Windows. The relative standard deviation was 11% (UK NEQAS for Lead & Cadmium in Blood Wolfson EQA Laboratory). The data were analyzed by use of the ***F***-test (95% confidence level, $\boldsymbol{k}$ = 1.96). Here $\boldsymbol{k}$ is the coverage factor applied to provide a confidence interval of ~95%, selected from the ***t***-distribution tables.

Measuring Size Distributions of Airborne Lead Containing Particles

It is well established that the deposition efficiency in lungs is influenced by the size of particles and forms a V-curve comprising two branches caused by two main mechanisms of particle deposition: diffusion for smaller particles (diameter < 200 nm) and inertial deposition for larger particles for diameters greater than 300 nm, e.g., Wilson *et al.* (1985); Schiller *et al.* (1988); ICRP (1994), Jaques and Kim (2000). According to expressions (2) and (3) it is necessary to use the sizes that correspond to the diffusion deposition (diffusivity equivalent size) for small particles and the aerodynamic size for large particles. There is only one instrument on the market that uses both sizes and, therefore, emulates the natural deposition in the respiratory system Nano ID Select.

This unique instrument (Nano-ID Select, Particle Measuring Systems) has been employed to collect airborne particles in a wide range of aerosol particle diameters from 2.5 nm to 30 μm. Aerosol particles were collected in 11 size fractions at a flow rate 20 L/min and a relative humidity of 80%. Sampling at a controlled humidity is an important feature of the Nano-ID Select instrument that enables conditions in the respiratory system to be emulated. Therefore, deposition within the instrument occurs under the same effective humidity as in human respiratory system. This reduces the effect of water uptake on the particle size distribution measurements.

Airborne particle size distributions $f_a(D_i)$ were calculated using measurements of mass collected at various size stages ($1 \le I \ge 11$), e.g., Hinds (1999):

$$f_a(D_i) = C_i/(\log D_{i+1} - \log D_i) \quad (4)$$

C_i is concentration of lead in μg/m^3 in air collected at i-stage: $C_i = m_i/Qt$ (Q is the flow rate through the instrument in m^3/min and t - the sampling time in minutes).

RESULTS AND DISCUSSION

Size Distributions of Lead at Working Places

The total mass concentration of lead aerosols determined at working places ranged from 0.6 μg/m^3 to 50 μg/m^3. The nanoparticle mass fraction of aerosols (sizes less than 100 nm) was found to vary from 10% to 60%.

A typical aerosol size distribution of lead (sampled in cutting and grinding areas at a factory) is shown in Fig. 4(a). The size distribution has a maximum at about 2 μm. In addition, there is a noticeable amount of lead associated with nanoparticles in the range from 0.01 to 0.1 μm. This

finding shows the importance of size-resolved monitoring nanoparticles because a considerable proportion of lead containing particles are in the nano-size range.

An aerosol sampled at Industrial Partner 2 contains more than 60% of Pb mass in the region of nanoparticles (Fig. 4(b)). Nanoparticles have very high respiratory tract deposition efficiency especially in the alveolar region, Finlay and Martin (2008). Thus, size-resolved sampling is crucial in evaluation of the health risk in occupational hygiene and air quality assessment at working places.

Number size distributions are interesting for health risk evaluation. Size-resolved chemical analysis provides a unique opportunity to calculate size distributions of a specific element, e.g., Pb. Mass distributions can be used for evaluation of number size distributions. However, this is not a straightforward procedure because of unknown morphology of particles and chemical architecture. It was assumed that lead particles form fractal structures with the fractal dimension Df = 2.7, see e.g., Aerosol Measurement (2001). The dN/dlogdp number size distribution was calculated according to expression dN/dlogdp = dm/dLogdp/m0, where dm/dLogdp is the mass size distribution, $m0 = (4/3\pi)\cdot\rho\cdot(dp/2)^{Df}$. The density ρ was equal to 11.35 g/cc. The number particle size distribution shows a single maximum at 5 nm, Fig. 4(c). This confirms importance of nanoparticles for lead aerosols.

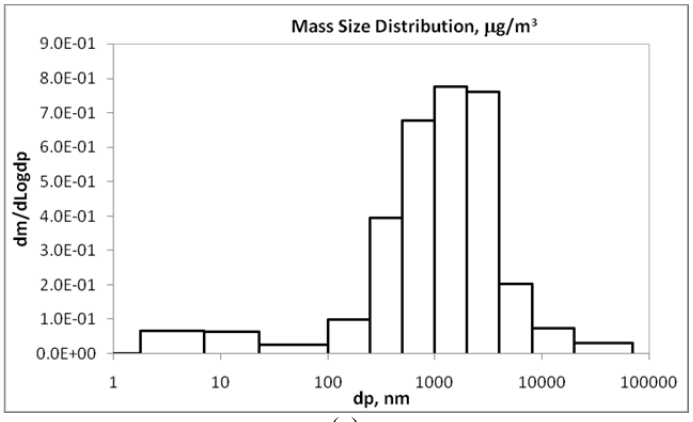

(a)

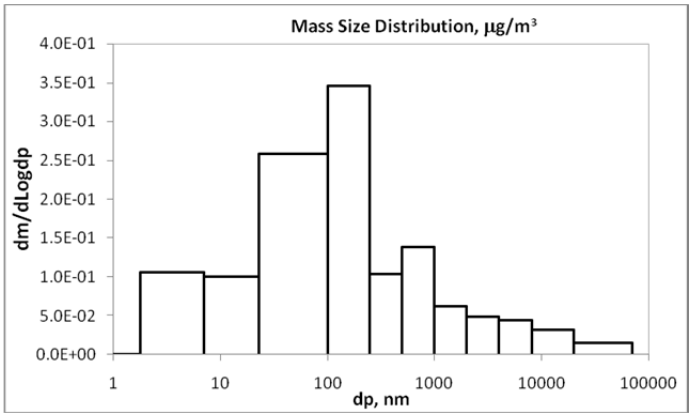

(b)

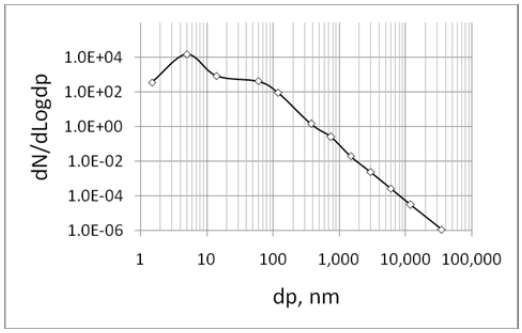

(c)

Fig. 4. Lead aerosol particle mass size distribution (dm/dlogdp) obtained at a factory processing lead. A typical size distribution of Pb obtained in cutting and grinding areas (a) and in a smelting area (b). Aerosol particle number size distribution (dN/dlogdp) obtained from Fig. 4(b).

Another important feature of the lead aerosol size distributions is its multi-modal structure. It indicates two major sources of lead: nucleation of primary lead aerosol particles from lead vapour (nanoparticle mode) and attrition processes (coarse mode).

The size distributions of aerosols very often are bi-modal. Bi-modal aerosol size distributions of lead in the size range from 0.25 μm to 50 μm were observed earlier by Tsai *et al.* (1997). However, bimodal distributions in the nano-size range have not been observed before.

Finally, it has to be pointed out that lead nanoparticles represent a considerable proportion of lead mass in the air of a factory that involves heating of lead or its compounds. Size resolved sampling shows wide variations in the size distributions including the total mass, number of modes, mean mass diameter of modes and proportion of micro- and nano- fractions of airborne particle size distributions. This confirms the importance of reliable measurements of size distributions in the entire size range of particulate matter including both micro- and nano- fractions for evaluation of air quality at working places.

ICRP Bio-Kinetic Model for Lead

A validated kinetic model of lead metabolism in humans is described in Appendix A.

Importance of the Respiratory Tract Deposition Efficiency – the First Fraction of HR-AD Model

An illustration of the importance of E(D) function for evaluation of health effects can be seen in results of modelling of bio-kinetics of lead due to exposure to airborne lead aerosols of various mass median diameters MMD. Calculations were performed with the same mass concentration of lead in the air but different MMD using the bio-kinetic model and expressions (2) and (3). The standard geometric deviation that represents the width of distributions σ_g was assumed to be 1.6. The total mass of lead to have entered the body was found from the integral of the size distribution over the size range of particles.

It clearly shows (Table 1) the link between the mean diameter of airborne particles and the blood level of lead accumulated. The exposure to nanoparticles of 10 nm will cause greater blood level and consequently more potential health risk than exposure to 100 nm or 1 μm particles. Even greater deposition was obtained for 10 μm particles. Thus, neglecting the deposition efficiency can cause considerable overestimation in the body burden and the health risk. However, it should be mentioned that the health risk associated with these large particles is not necessarily very prominent due to other factors discussed later.

Evaluation of the Fraction of Lead Staying in the Body Compartments and Causing the Adverse Health Effects (Biological Availability of Lead Particles)

Airborne particle size distributions along with the bio-kinetic model and the respiratory system deposition efficiency enable the fraction of particles causing adverse health effects $A(D)$ to be evaluated. The blood lead content was calculated using aerosol particle size distributions in three stages. First, airborne lead mass size distributions $f_a(D)$ were obtained with Nano-ID Select samplers. Second, deposited aerosol mass distributions were calculated using known efficiency of deposition particles in the respiratory tract $E(D)$, see expression (1). Finally, these distributions were multiplied by $A(D)$ and the total bio-available mass of lead was fed into the bio-kinetic numerical computation code to produce the calculated blood lead content. The calculated values of lead in the blood were compared with the measured ones for various $A(D, par)$ to find the best fit mode parameters.

Every $A(D)$ model generated certain levels of lead in the blood of workers. Several simple models of bio-availability were considered. The first model is a non-size selective model. It is described by a single parameter that represents a fraction of bio-available lead (the same over the entire particle size range). Two size-selective models were considered. For simplicity, these were based on the concept of the critical particle size D_c. In the second model, it was assumed that particles of greater diameters than D_c could be bio-available but smaller particles removed by unknown means. In the third model we assumed that particles of smaller diameters than D_c dissolved in the lung fluid, therefore lead became bioavailable, but the larger particles ($D > D_c$) could not be dissolved and were eventually removed by cleaning mechanisms. In addition, small particles stay longer in the lung due to alveolar deposition and consequently prolonged retention causes slower clearance.

In this way concentration of lead in the blood of workers C_{cal} was found using airborne particles size distributions obtained at the factories. Then calculated concentrations of lead in blood were compared to the measured lead blood content C_{meas}.

Results Obtained for Various Models A(D)

In the first run we used a non-size selective model, with the assumption that 95% of the mass of all deposited in the respiratory system particles would be absorbed directly into blood ($E(D) = 0.95$). The deposition fraction of Pb aerosol particles in the lung was taken from ICRP (1994).

Calculated blood level concentrations obtained with the non-size selective model showed very little agreement with

Table 1. Concentration of Pb after 10 years of exposure to aerosols of various mass median diameter MMD and total mass concentration 1 μg/m^3.

MMD, nm	m_{50}, TOTAL IN BODY, μg	IN BLOOD, ng/dl
10	783	333
100	174	74
1000 (1 μm)	348	148
10000 (10 μm)	870	370

the experimental data. The regression analysis revealed a poor correlation between calculated and measured lead concentrations: $R^2 = 0.387$. For instance lead concentrations in blood measured in Industrial Partner 1 and Industrial Partner 2 are considerably higher than calculated ones whilst measured concentration at Industrial Partner 3 was lower than the calculated value.

The background lead concentration was assumed to be about 0.2–0.4 μg/m^3 (Tsai *et al.*, 1997). It was found that taking into account the background lead concentration did not reduce the disparity between calculated and observed levels of lead in blood.

Calculations were also performed with the model assuming different proportions of lead absorbed into blood. It was found that variations of the bio-available proportion from 0 to 100% did not help to increase correlation between calculated and measured data ($R^2 < 0.4$).

Another source of disagreement between calculated and observed levels could be dietary lead entering via the gastrointestinal tract, for instance with food, drinks, etc. (e.g., Gross, 1981). To test this dietary lead consumption was included in the first model as an independent parameter. Calculations of the first model including dietary intake did not show much improvement in correlation (Fig. 5). Therefore, the non-size selective model of bio-availability is not supported by experimental results.

In the second model D_c was used as an unknown parameter along with the background concentration associated with lead consumption via non-lung pathways. This model might be relevant to highly fractal agglomerated particles. Solubility of such fractal structures is likely to be the same for different sizes but the mass of soluble bio-available material will be greater for larger particles. This may or may not be the case for lead but it is difficult to disregard this option completely. The absorbed amount of lead from aerosol by a human body was calculated from the aerosol size distribution $f_a(D,)$ the deposition fraction $E(D)$ and the bio-availability function $A(D)$:

$$M_i = \int_{-\infty}^{\infty} f_{ai}(D)E(D)A(D)d\log D = \int_{\log D_c}^{\infty} f_{ai}(D)E(D)d\log D, \quad (5)$$

where M_i is the absorbed (bio-available) mass of lead for i-size distribution. Values of M_i were used to calculate (using the bio-kinetic model) the blood lead concentration for i-size distribution C_{Bic}. D_c was found by minimising the difference between measured blood lead C_{Bim} and calculated concentrations:

$$Min\sum_{i=1}^{6}\left[C_{Bim} - C_{Bic} - C_{gt}\right]^2, \quad (6)$$

where C_{gt} is the lead concentration associated with the consumption of lead through non-lung pathways. Expression (6) was used to find both D_c and C_{gt}.

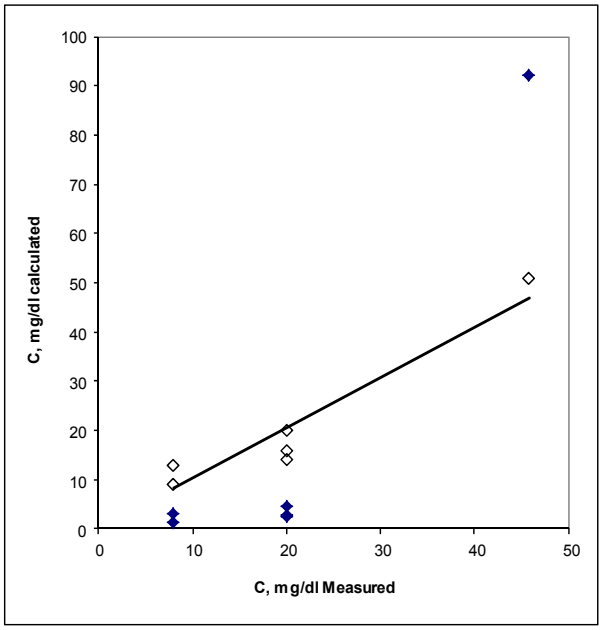

Fig. 5. Calculated and measured concentrations of blood lead in workers at various plants. Dark diamonds - the first non-size selective model with the dietary lead consumption included. White diamonds - the size-selective model with $D_c = 200$ nm.

Regression analysis revealed a poor correlation between measured and calculated blood lead content for the second model. The R^2 was even less than for the non-size selective model.

In the third model mass was calculated using expression (7) that was similar to one used for the second model (8):

$$M_i = \int_{-\infty}^{\log D_c} f_{ai}(D)E(D)d\log D, \quad (7)$$

The solution of expression (7) gives value for $D_c = 0.2$ μm and 12.0 μg/dl for C_{gt}. The difference between calculated and measured values was small (see Fig. 5). Therefore, the third model shows a good agreement between experimental data on lead in blood and calculated with the ICRP model and aerosol size distributions of lead at workplaces.

There are several possible reasons for size-dependent nature of bio-availability. Firstly, solubility of particles is influenced by their size. It is known that nanoparticles are more soluble than the bulk material. This is due to the effect of the surface free energy term on the equilibrium of a particle in the liquid. The surface term is always positive and this increases the free energy of nanoparticles in comparison to the free energy of the solution. The surface term is proportional to D^{-1}, therefore, it is possible to find such a value of D that makes nanoparticles unstable in liquids. The enhanced solubility of nanoparticles is well known phenomenon. For example, small nanoparticles of SiO_2 can be dissolved in water according to Larson *et al.* (2010).

Another cause of the origin of D_c is clearance by the mucociliary escalator of the respiratory system. Larger

particles are removed from the respiratory tract faster than nanoparticles because smaller and larger particles are deposited into different regions of the respiratory tract Oberdörster *et al.* (1994); Asgharian *et al.* (2001); Kleinstreuer *et al.* (2008). Swallowing of particles from lung clearance potentially may bring these particles into the blood stream. This mechanism is not very well understood/quantified but it is unlikely to be of major importance. The retention time in the GI-tract is about 1 day in comparison to weeks and months for the respiratory tract and especially alveolar region, Leggett (1993). Therefore, swallowed particles have higher probability to be excreted than to be dissolved into the blood. The mechanism of the effect of particle sizes on the bio-availability is not well understood at the moment. However, it is clear that nanoparticles and micro-size particles of lead have different bio-availability.

It is important to point out that toxicity of airborne lead is associated mainly with smaller particles (D < 200 nm), see Fig. 4. Thus, at working places and in general environment this fraction of airborne lead is the subject of major concern and should be considered most dangerous for health. It is also practical and may be cost effective to concentrate, at working places, on eliminating the sources of this fraction of airborne lead particles instead of spending resources on cleaning all the possible sources of airborne lead.

It is interesting to evaluate the performance of the NR-AD approach with different (not optimised) values of D_c corresponding to some suggested earlier fractions of the particulate matter as a measure of health risk. PM_{10}, $PM_{2.5}$ and later PM_1 were used for characterisation of health risk associated to exposure to airborne particles, Hinds (1999). Results of regression analysis of the second model with these values of D_c are shown in Table 2.

Table 2 reveals a poor correlation for the PM_{10} fraction (R^2 < 0.36), for $PM_{2.5}$ (R^2 < 0.68) and PM_1 (R^2 < 0.72). These are considerably lower than R^2 value for D_c = 200 nm (R^2 = 0.91). Thus, for the lead aerosols measured, the health risk would seem to be associated with the inhalation of the ultra-fine fraction of the aerosol (D_c < 200 nm) rather than with the coarser fractions.

A good illustration of the importance of two-fraction concept for the HR-AD approach and hence for the health risk evaluation can be seen comparing lead mass: in the air, captured by the respiratory system and captured by the body, Fig. 6. First, the fraction of the mass concentration deposited in the respiratory system $E(D)$ is a half of the mass concentration of lead particles in the air (compare white and grey bars). It should be pointed out that this ratio is the size sensitive. Even greater effect of the second fraction $A(D)$ can be observed. The fraction of mass remaining in the body and, therefore, responsible for the adverse health effects (black) is close to the fraction captured by the respiratory system for small particles (range of particle sizes from 23 to 100 nm). However, for the larger particles (the size range of from 2,000 to 4,000 nm) the black fraction (responsible for adverse health effects) is almost zero. Thus, at each stage corresponding to the first and the second fraction the mass available to cause the adverse health effects is smaller but the degree of bioavailability is not constant and is influenced by the particle size.

In the past there were several publications suggesting the higher risk associated with nanoparticles. In this paper, this is quantified and explained by a combination of effects of the size selective deposition in the respiratory tract and removal from the body by cleaning mechanisms.

CONCLUSIONS

The total mass concentration of lead aerosols determined at working places ranged from 0.6 μg/m^3 to 50 μg/m^3. The nanoparticle mass fraction of aerosols (sizes less than 0.1 μm) was found to vary from 10% to 60%. The fraction of lead remaining in the body (responsible for adverse health effects) has been determined. It was found that lead particles with the diameter below 200 nm cause adverse health effects but larger particles do not cause any measurable health effect. The evaluation of health risk based upon PM_{10}, $PM_{2.5}$ or PM_1 fractions does not provide correct blood lead content. It is found that PM_{10}, $PM_{2.5}$ or PM_1 will overestimate the health risk considerably. It was shown that the approach proposed for health risk evaluation based on quantification of amount of particulate matter of concern captured by body provides valuable information for health risk assessment and air quality control at working places. Authors believe that in the future quantification of exposure to airborne nanomaterials should be based upon size resolved chemical composition data measured over the wide size range including nanoparticles as well as micron size particles, regional airway deposition efficiencies and evaluation of the bioavailability.

ACKNOWLEDGMENTS

This study was supported in parts by EU Project "Evaluation of the biosafety of lead substitutes used in the manufacture of unleaded crystal glass" (BRST-CT97-5122).

APPENDIX A

ICRP Bio-Kinetic Model for Lead

A validated kinetic model of lead metabolism in humans (ICRP, 1975; Leggett, 1993) was employed to predict blood-lead levels in workers exposed to lead aerosols with size distributions equivalent to those collected in the work places.

Table 2. Results of the regression analysis.

Third model of $A(D)$ with various D_c	R^2	Average ratio, C_{cal}/C_{meas}
10 μm (PM_{10})	0.36	1.25
2.5 μm ($PM_{2.5}$)	0.68	1.19
1 μm (PM_1)	0.72	1.15

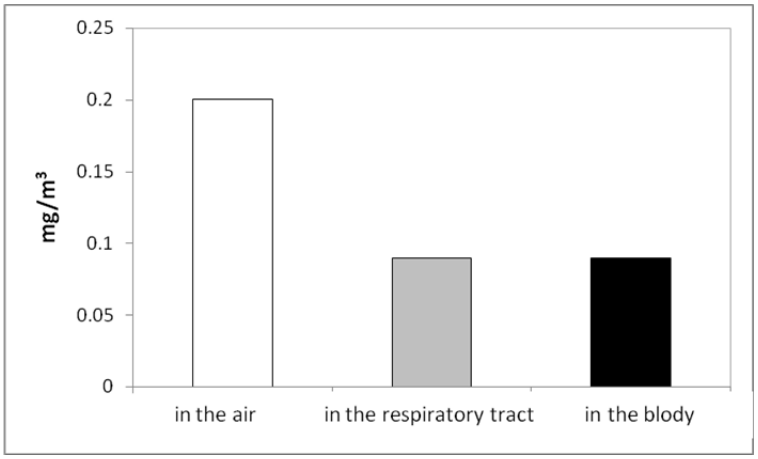

(a)

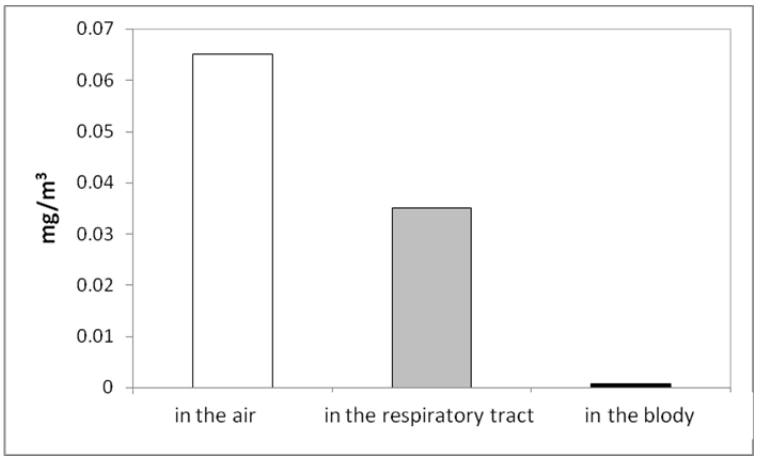

(b)

Fig. 6. Mass concentration of lead particles in the air (white rectangular), the fraction of the concentration deposited in the respiratory system (grey) and the proportion responsible for the adverse health effects black (remaining in the body). Mass concentration is in mg/m^3. (a) Data for the size range of particles from 23 to 100 nm (furnace area). (b) Data for the size range of particles from 2,000 to 4,000 nm (furnace area).

The model enables the blood lead concentration to be linked with lead concentration in the air. It was a comprehensive size resolved model that accounts for the body intake and the exchange between various bodycompartments.

The biokineticmodel for lead Leggett (1993) is a 27-compatment model, see Fig. 7. The model enables evacuation of lead with sweat, urine and excreta to be calculated along with contents in various body compartments. The model contains a set of transfer rate constants between the compartments. For instance, k_{ij} is the constant that describes the transfer rate from i-compartment to j-compartment:

$$\frac{dm_i}{dt} = -k_{ij} m_i , \tag{5}$$

where m_i is the mass of lead in the i-compartment and t is the time. This equation is similar to an equation for a chemical reaction of the first order. Eq. (5) has the solution:

$$m_i = m_{i(t=0)} e^{-k_{ij} t} , \tag{6}$$

where $m_{i(t\,=\,0)}$ is the value of m_i at $t = 0$. If $k_{ij}t < 1$ then a linear relationship between the mass and the time could be obtained from (6):

$$\Delta m_{ij} = m_{i(t\,=\,0)} - m_i = m_{i(t\,=\,0)}\, k_{ij} t , \tag{7}$$

where Δm_{ij} is the mass transferred from i-compartment into j-compartment. Expression (7) was used in a computer program implementation of the model. The computer program has been developed for Windows platform using C^{++}. It was developed to be run on a PC. The set of constants is shown in Table A1 in the Annex.

The program is based upon the direct integrating of the kinetic equations between compartments. This method requires relatively large computing resources however direct integrating has one important advantage: it enables calculations for a complex intake pattern of a toxic substance. Thus, the program can be used to run the bio-kinetic model with either zero or lower intake, for example during holidays and weekends.

The transfer rate from the small intestine to the large

intestine (k_{sl}) was calculated as the ratio of the product to the sum of the transfer rates from the small intestine to the upper large intestine (7) and from the upper large intestine to the lower large intestine (1.8), see Leggett (1993). It was found that k_{sl} = 1.4. Thus, this constant was calculated as a combination of two successive chemical reactions.

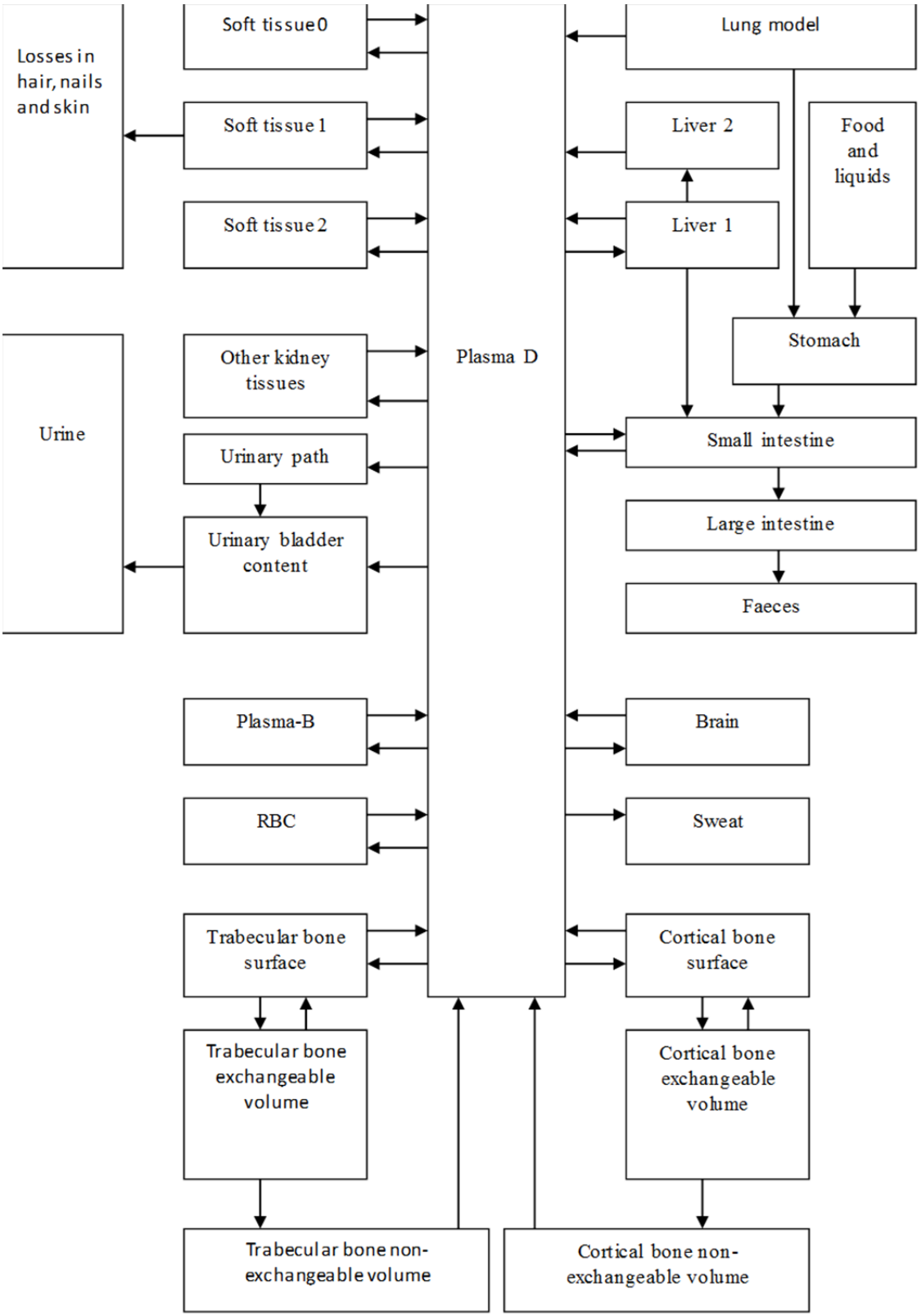

Fig. 7. Biokinetic model for lead (Leggett, 1993). RBC – red blood cells. Plasma B represents white blood cells. Plasma D represents the plasma without red and white blood cells.

Table A1. Transfer constants between body compartments per day for lead.

	Source compartment and destination compartment	Transfer rate, day^{-1}
1	Plasma-D to red blood cells (RBC)	480
2	Plasma-D to urinary bladder	30
3	Plasma-D to small intestine	12
4	Plasma-D to trabecular bone surface	88.96
5	Plasma-D to cortical bone surface	71.0
6	Plasma-D to liver 1	80
7	Plasma-D to kidneys urinary path	40
8	Plasma-D to kidneys other tissues	0.4
9	Plasma-D to soft tissue 0	177.5
10	Plasma-D to soft tissue 1	10.0
11	Plasma-D to soft tissue 2	2.0
12	Plasma-D to sweat	7.0
13	RBC to Plasma-D	0.139
14	Cortical bone surface to Plasma-D	0.5
15	Trabecular bone surface to Plasma-D	0.5
16	Cortical surface to exchangeable bone volume (XBV)	0.5
17	Trabecular bone surface to XBV	0.5
18	Cortical XBV to bone surface	0.0185
19	Trabecular XBV to bone surface	0.0185
20	Cortical XBV to nonexchangeable bone volume	0.00462
21	Trabecular XBV to nonexchangeable bone volume	0.00462
22	Cortical nonexchangeable volume to Plasma-D	$8.22\ 10^{-5}$
23	Trabecular nonexchangeable volume to Plasma-D	$4.93\ 10^{-4}$
24	Liver 1 to Plasma-D	0.0312
25	Liver 1 to small intestine	0.0312
26	Liver 1 to liver 2	0.00693
27	Liver 2 to Plasma-D	0.0019
28	Urinary path to urinary bladder	0.139
29	Kidneys (other tissue) to Plasma-D	0.0019
30	Soft tissue 0 to Plasma-D	2.079
31	Soft tissue 1 to Plasma-D	0.00416
32	Soft tissue 1 to losses	0.00277
33	Soft tissue2 to Plasma-D	0.00038
34	Plasma-D to brain	0.3
35	Plasma-B to Plasma-D	0.139
36	Brain to Plasma-D	0.00095
37	Plasma-D to Plasma-B	0.8
38	Small intestine to Plasma-D	0.225
39	Stomach to small intestine	24
40	Small intestine to large intestine	1.4
41	Large intestine to feces	1

The extravascular fluid compartment (EVF) has not been included into the model because the transfer rates from plasma-D to EVF and from EVF to plasma-D are very high 1000 and 333.3 respectively. Thus, these rates are important only in a relatively short-term scale: minutes (Leggett, 1993). The mass of blood of reference man has been assumed to be 5.4 kg and the volume of air breathed in during 8hr-shift (light work) - 9600 litres (ICRP, 1975). The program code has been verified using published data. According to ICRP model (Leggett, 1993), 1 day after administration of lead, blood typically contains 55–60% of the injected amount. Our program gives 57% of blood lead at 1 day. In addition, the code was verified using data on exposed volunteers to lead oxide aerosols obtained by Griffin *et al.* (1975). The difference between measured lead concentrations in blood after 100 days of exposure and calculated with the code was less than 10%. Thus, the program provides good agreement with existing published data.

The code has also been verified using data on lead in blood obtained by Rabinowitz *et al.* (1976). In these experiments, lead was introduced to adult human subjects during a period of about 100 days. Maximal value of lead blood content was found to be close to 35 μg/dl. Calculated curves obtained with the code developed were in a good agreement with experimental data, see Fig. 8. Lead is a bone-seeking element O'Flaherty (1993). This behaviour is caused by long-term kinetics associated with absorption of lead by bones.

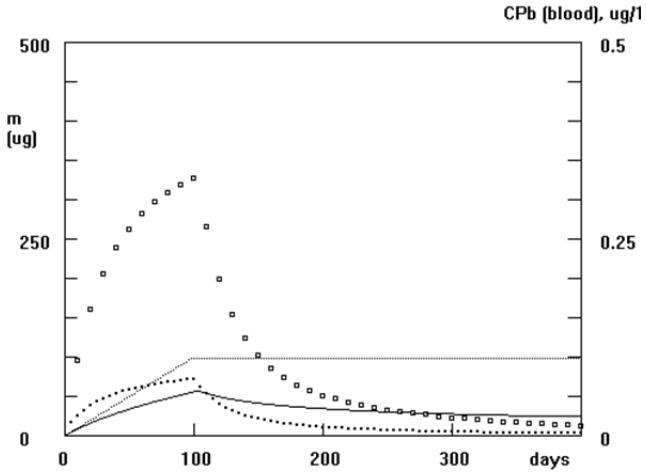

Fig. 8. Calculations of lead content after 1 μg lead intake into plasma-D every day during the first 100 days. Total Pb in the body in μg - solid line (the left scale). Total Pb administered - dotted line (the left scale). Concentration of lead in blood in μg/dl - large rectangles (the right scale). Urine per day in μg - small rectangles (the left scale multiplied by 10).

REFERENCES

Anjilvel, S. and Asgharian, B. (1995). A Multiple-Path Model of Particle Deposition in the Rat Lung. *Fundam. Appl. Toxicol.* 28: 41–50.

Asgharian, B., Hofmann, W. and Bergmann, R. (2001). Particle Deposition in a Multiple-Path Model of the Human Lung. *Aerosol Sci. Technol.* 34: 332–339.

Baron, P.A. and Willeke, K. (2001). *Aerosol Measurement. Principles, Techniques and Applications.* J. Wiley and sons, p. 1131.

Brown, J.S., Zeman, K.L. and Bennett, W.D. (2002). Ultrafine Particle Deposition and Clearance in the Healthy and Obstructed Lung. *Am. J. Respir. Crit. Care Med*. 166: 1240–1247.

Chamberlain, A.C. (1985). Prediction of Response of Blood Lead to Airborne and Dietary Lead from Volunteer Experiments with Lead Isotopes. *Proc. R. Soc. London, Ser. B* 224: 149–182.

Dockery, D.W., Pope, C.A., Xu, X., Spengler, J.D., Ware, J.H., Fay, M.E., Ferris, B.G. and Speizer, F.E. (1993). An Association between Air Pollution and Mortality in Six US Cities. *New Engl. J. Med.* 329: 1753–1759.

Donaldson, K., Li, X.Y. and MacNee, W. (1998). Ultrafine (Nanometer) Particle-Mediated Lung Injury. *J. Aerosol Sci*. 29: 553–60.

Ferin, J., Oberdorster, G. and Penny, D.P. (1992). Pulmonary Retention of Ultrafine and Fine Particle in Rats. *Am. J. Respir. Cell Mol. Biol.* 6: 535–542.

Ferin, J. (1994). Pulmonary Retention and Clearance of Particles. *Toxicol. Lett.* 72: 121–125.

Finlay, W.H. and Martin, A.R. (2008). Recent Advances in of Predictive Understanding of Respiratory Tract Deposition. *J. Aerosol Med. Pulm. Drug Deliv.* 21: 189–205.

Gnewuch, H., Muir, R., Gorbunov, B., Priest, N.D. and Jackson, P.R. (2009). A Novel Size-Selective Airborne Particle Sampling Instrument (WRAS) for Health Risk Evaluation, In *Nanomaterials: Risk and Benefits*. Linkov, I. and Steevens, J. (Eds.), Springer, The Netherlands, p. 225–233.

Gorbunov, B., Priest, N.D., Muir, R.B., Jackson, P.R. and Gnewuch, H. (2009). A Novel Size-Selective Airborne Particle Size Fractionating Instrument for Health Risk Evaluation. *Ann. Occup. Hyg.* 53: 225–237.

Gorbunov, B., Muir, R., Bello, D., Gnewuch, H., LeCloux, A., Luizi, F., Del Tedesco, M. and Green, D. (2010) Exposure - Dose Relationship for Airborne Nanoparticles. In *Advances in Environmental Research*, *Volume 4*, Daniels, J.A. (Ed.), Nova Publishes.

Griffin, T.B., Coulston, F., Wells, H., Russell, J.C. and Knelson, J.H. (1975). Clinical Studies of Men Continuously Exposed to Airborne Particulate Lead. In *Lead*, Griffin, T.B. and Knelson, J.H. (Eds.), Acad. Press, N.Y., p. 221–239.

Gross S.B. (1981). Human oral and Inhalation Exposures to Lead: Summary of Kehoe Balance Experiments. *J. Toxicol. Environ. Health* 8: 333–377.

Hinds, W.C. (1999). *Aerosol Technology. Properties, Behaviour and Measurement of Airborne Particles*. J. Wiley and Sons, N.Y., p. 233–259.

Holbrook, L.T. and Longest, P.W. (2013). Validating CFD Predictions of Highly Localized Aerosol Deposition in Airway Models: *In Vitro* Data and Effects of Surface Properties. *J. Aerosol Sci.* 59: 6–21.

ICRP - International Commission on Radiological Protection (1975). Report of Task Group on Reference Man/ Oxford: Pergamon Press.

ICRP (1994). International Commission on Radiological Protection.Human Respiratory Tract Model for Radiological Protection. Annals of the ICRP, Publication 66, Tarrytown, Elsevier Science Inc., N.Y.

Jaques, P.A. and Kim, C.S. (2000). Measurement of Total Lung Deposition of Inhaled Ultrafine Particles in Healthy Men and Women. *Inhalation Toxicol.* 12: 715–731.

John, W. (2001). Size Distribution Characteristics of Aerosols, In *Aerosol Measurement. Principles, Techniques and Applications*, Baron, P.A. and Willeke, K. (Eds.), J. Wiley and Sons, N.Y., p. 99–116.

Kleinstreuer, C., Zhang, Z. and Li, Z. (2008). Modelling Airflow and Particle Transport/Deposition in pulmonary Airways. *Respir. Physiol. Neurobiol.* 163: 128–138.

Koch, W. and Stöber, W. (2001). A Simple Pulmonary Retention Model Accounting for Dissolution and Macrophage-Mediated Removal of Deposited Polydisperse Particles. *Inhalation Toxicol.* 13: 129–148.

Larson, R.R., Story, S.G. and Hegmann, K.T. (2010). Assessing the Solubility of Silicon Dioxide Particles Using Simulated Lung Fluid. *Open Toxicol. J.* 4: 51–55.

Leggett, R.W. (1993). An Age-Specific Kinetic Model of Lead Metabolism in Humans. *Environ. Health Perspect.* 101: 598–616.

Lippmann, M. (1995) Size-selective health hazard Sampling, In *Air Sampling Instruments for Evaluation of*

Atmospheric Contaminants, 8th Ed., ACGIH, Cincinnati.

Nemmar, A, Hoet, P.H.M., Vanquickenborne, B., Dinsdale, D., Thomeer, M., Hoylaerts, M.F., Vanbilloen, H., Mortelmans, L. and Nemery, B. (2002). Passage of Inhaled Particles into the Blood Circulation in Humans. *Circulation* 105: 411–414.

Oberdorster, G., Ferin, J. and Lehnert, B.E. (1994). Correlation between Particle-Size, in-Vivo Particle Persistence, and Lung Injury. *Environ Health Perspect*. 102: 173–179.

O'Flaherty, E.J. (1993). Physiologically Based Models for Bone-Seeking Elements. *Toxicol. Appl. Pharmacol.* 118: 16–29.

Peters, A., Wichmann, H.E., Tuch, T., Heinrich, J. and Heyder, J. (1997). Respiratory Effects are Associated with the Number of Ultrafine Particles. *Am. J. Respir. Crit. Care Med*. 155: 1376–1383.

Phalen, R.F., Oldham, M.J. and Nel, A.E. (2006) Tracheobronchial Particle Dose Concentrations for *in Vitro* Toxicology Studies. *Toxicol. Sci.* 92: 126–132.

Pope, C.A., Dockery D.W. and Schwartz, J. (1995). Review of Epidemiological Evidence of Health Effects of Particulate Air Pollution. *Inhalation Toxicol.* 7: 1–18.

Rabinowitz, M.B., Wetherill, G.W. and Kopple, J.D. (1976). Kinetic Analysis of Lead Metabolism in Healthy Humans. *J. Clin. Invest*. 58: 260–270.

Schiller, C.F., Gebhart, J., Heyder, J., Rudolf, G. and Stahlhofen, W. (1988). Deposition of Monodisperse Insoluble Aerosol Particles in the 0.005 to 0.2 μm Size Range within the Human Respiratory Tract. *Ann. Occup. Hyg*. 32: 41–49.

Seaton, A., MacNee, W., Donaldson, K. and Godden, D. (1995). Particulate Air Pollution and Acute Health Effects. *Lancet* 345: 176–178.

Tsai, C.J., Shih, T.S. and Sheu, R.N. (1997). Characteristics of Lead Aerosols in Different Work Environments. *Am. Ind. Hyg. Assoc. J.* 58: 650–656.

Whitby, K.T. (1978). The Physical Characteristics of Sulphur Aerosols. *Atmos. Environ.* 12: 135–159.

Wilson, F.J.Jr., Hiller, F.C., Wilson, J.D. and Bone, R.C. (1985). Quantitative Deposition of Ultrafine Stable Particles in the Human Respiratory Tract. *J. Appl. Physiol.* 58: 223–229.

Xi, J. and Longest, P.W. (2008). Evaluation of a Novel Drift Flux Model for Stimulating Sub-Micrometer Aerosol Dynamics in Human Upper Tracheobronchial Airways. *Ann. Biomed. Eng.* 36: 1714–1734.

Yeh, H.C., Cuddihy, R.G., Phalen, R.F. and Chang, I.Y. (1996). Comparisons of Calculated Respiratory Tract Deposition of Particles Based on the Proposed NCRP Model and the New ICRP Model. *Aerosol Sci. Technol.* 25: 134–140.

Received for review, February 5, 2013
Accepted, June 5, 2013